On the Vibrational linear and nonlinear optical properties of compounds involving noble gas atoms: HXeOXeH, HXeOXeF, and FXeOXeF

ARTICLE *in* JOURNAL OF COMPUTATIONAL CHEMISTRY · JUNE 2013

Impact Factor: 3.59 · DOI: 10.1002/jcc.23280 · Source: PubMed

4 AUTHORS, INCLUDING:

Aggelos Avramopoulos
National Hellenic Research Foundation
54 PUBLICATIONS **569** CITATIONS
SEE PROFILE

Heribert Reis
National Hellenic Research Foundation
77 PUBLICATIONS **983** CITATIONS
SEE PROFILE

Josep M. Luis
Universitat de Girona
106 PUBLICATIONS **2,461** CITATIONS
SEE PROFILE

On the Vibrational Linear and Nonlinear Optical Properties of Compounds Involving Noble Gas Atoms: HXeOXeH, HXeOXeF, and FXeOXeF

Aggelos Avramopoulos,*[a] Heribert Reis,[a] Josep M. Luis,[b] and Manthos G. Papadopoulos[a]

The vibrational (hyper)polarizabilities of some selected Xe derivatives are studied in the context of Bishop–Kirtman perturbation theory (BKPT) and numerical finite field methodology. It was found that for this set of rare gas compounds, the static vibrational properties are quite large, in comparison to the corresponding electronic ones, especially those of the second hyperpolarizability. This also holds for the dc-Pockels $\beta(-\omega;\omega,0)$, Kerr $\gamma(-\omega;\omega,0,0)$ and electric field second harmonic generation γ $(-2\omega;\omega,\omega,0)$ effects, although the computed nuclear relaxation (nr) vibrational contributions are smaller in magnitude than the static ones. HXeOXeH was used to study the effects of electron correlation, basis set, and geometry. Geometry effects were found to lead to noticeable changes of the vibrational and electronic second hyperpolarizability. A limited study of the effect of Xe insertion to the nr vibrational properties is also reported. Assessment of the results revealed that Xe insertion has a remarkable effect on the nr (hyper)polarizabilities. In terms of the BKPT, this is associated with a remarkable increase of the electrical and mechanical anharmonicity terms. The latter is consistent with the anharmonic character of several vibrational modes reported for rare gas compounds. © 2013 Wiley Periodicals, Inc.

DOI: 10.1002/jcc.23280

Introduction

The history of noble gas chemistry has its roots in 1962 when Bartlet[1] and Hoppe[2] successfully synthesized and identified stable noble gas compounds. Since then a large number of experimental and theoretical groups have worked on the synthesis and elucidation of the nature of bonds involving Ng atoms (where Ng stands for noble gas).[3–5] Most of the synthesized compounds involved only Xe and Kr, as chemical inertness increases with decreasing atomic number of the Ng atom.[5,6] A new type of molecule of the form HNgY, where Y is an electronegative atom or group of atoms that has been synthesized. Examples of these derivatives are HArF, prepared by Khriachtchev et al.,[7] HXeH synthesized by Feldman et al.[8], and HKrF reported by Pettersson et al.[9] This class of molecules was prepared by photolysis of Hartree–Fock (HF) in a Ng matrix at low temperature and identified with the aid of vibrational spectroscopy. The above species have been shown to exhibit a large charge transfer character, the H—Ng bond is predominantly covalent and Ng–Y has a substantial ionic contribution.[4,10,11] An extensive literature survey on the chemistry of rare gas molecules can be found in Refs. [4] and [12].

Among the most remarkable developments in the chemistry of noble gas compounds, one may note: (i) the synthesis of fluorine-free organoxenon derivatives[13,14] and covalent C_6F_5XeF and C_6F_5XeCN compounds[15]; (ii) the X-ray crystal structures of the $[Xe_3OF_3][PnF_6]$ salts, where Pn = As, Sb, which contain the Z-shaped $FXeOXeFXeF^+$ cation[16] and $[H_3O][PnF_6]\cdot 2XeF_2$ in which the XeF_2 molecules interact with the H_3O^+ cations; (iii) the formation of XeO_2 at 0°C by hydrolysis of XeF_4 in water,[17] HXeOH in low temperature Xe matrix,[18] and the neutral radical HXeO[19]; (iv) a metal–Xenon compound involving the Xe—Au bond[20,21]; and (v) the recent synthesis of halogenated xenon cyanides.[22]

Much less is known about derivatives involving the Ng—Ng bond. Seppelt reported the isolation of a salt with the cation Xe_2^+, that has a Xe—Xe bond of 3.087 Å.[23] However, Khriachtchev et al.[24] reported the synthesis of HXeOXeH, which contains two Xe atoms. Apart from the synthesis and identification of rare gas compounds, a number of theoretical groups have reported studies on the stability, formation mechanisms, structure, and bonding nature of several rare gas compounds.[5,6,25–35]

We have reported that insertion of an Ng atom remarkably enhances the nonlinear response of the resulting derivative.[36] This has been attributed to the noteworthy lowering of the excited states accompanied by more intense allowed electronic transitions.[36,37] Recently, we reported that the diradical

[a] A. Avramopoulos, H. Reis, M. G. Papadopoulos
Institute of Biology, Medicinal Chemistry and Biotechnology, National Hellenic Research Foundation, Athens 116 35, Greece
[b] J. M. Luis
Institute of Computational Chemistry and Department of Chemistry, University of Girona, Campus De Montilivi, 17071, Girona, Catalonia, Spain
E-mail: aavram@eie.gr

Contract/grant sponsor: European Union's Seventh Framework Programme (FP7-REGPOT-2009-1, Project ARCADE); Contract/grant number: 245866; Contract/grant sponsor: High-Performance Computing Infrastructure for South East Europe's Research Communities (HP-SEE), cofunded by the European Commission through the Seventh Framework Programme; Contract/grant number: 261499.

character of HXe_2F has a remarkable effect on the linear and nonlinear optical (L&NLO) properties.[37] We have demonstrated that oxygen insertion between the two Xe atoms of AXeOXeB, where A,B = H,F, increases the stability of the formed species and decreases its nonlinear optical character.[38] The goal of these studies was to understand the mechanisms associated with the remarkable polarization properties of rare gas derivatives. This may be important also from a technological point of view, because materials with high NLO properties are required for the fabrication of devices with many technological applications.[39]

So far our previous studies have been focused mainly on the computation of the electronic part of the linear and nonlinear response of the considered Ng derivatives. However, it is known that vibrations may have a significant contribution to the static and dynamic (hyper)polarizabilities.[40,41] Several studies have discussed the role of the vibrational contributions to these properties and concluded that they can be of major importance.[42] A theoretical study of the vibrational spectrum of HXeOXeH revealed the anharmonic character of some vibrational modes.[24] The high anharmonic character of the Xe—H stretching mode has been also studied by the correlation-corrected vibrational self-consistent field method (CC-VSCF) combined with the second-order Møller–Plesset perturbation theory (MP2) level to compute the potential energy surface (MP2/CC-VSCF), in a series of HXeY molecules.[43,44] The aim of this study is to present the vibrational (hyper)polarizabilities of HXeOXeH, HXeOXeF, and FXeOXeF derivatives and to perform a comparative study with the corresponding electronic contributions. Elaboration of the results will assist us to study the effect of the vibrational anharmonic character of several modes, found in rare gas derivatives, on their (hyper)polarizabilities. Furthermore, the analysis of the electronic and vibrational hyperpolarizability will allow to gain a broader and complete understanding on the origin of the high polarization character of derivatives formed by rare gas insertion. This knowledge can be used for improving the design of new molecules with very large nonlinear optical properties.

Methods and Computational Details

Electronic L&NLO properties

When a molecule is subject to a uniform static electric field F, its energy, E, may be expanded as follows[45]:

$$E = E^0 - \mu_i F_i - (1/2)\alpha_{ij}F_iF_j - (1/6)\beta_{ijk}F_iF_jF_k - (1/24)\gamma_{ijkl}F_iF_jF_kF_l \ldots, \quad (1)$$

where E^0 is the field free energy of the molecular system, F_i, F_j, F_k, F_l are the field components, μ_i, α_{ij}, β_{ijk}, and γ_{ijkl} are the tensor components of the dipole moment, linear dipole polarizability, first and second hyperpolarizability, respectively. Summation over repeated indices is implied.

By using the finite difference method, the diagonal components of the polarizability (α_{ii}), first hyperpolarizability (β_{iii}), and second hyperpolarizability (γ_{iiii}) were obtained as the second-, third-, and fourth-order derivatives of the field-dependent energy, respectively. The Romberg approach[46] was used to safeguard the numerical stability of the results and to remove higher-order contaminations. A number of field strengths of magnitude 2^mF were used, where m = 0, 1, 2, 3, 4 and the base field F = 0.0008 a.u. For all the reported computations in this study, the molecules lie in the XZ plane (Fig. 1), and only the in-plane diagonal components of the electronic (hyper) polarizabilities were considered. All the reported electronic (hyper)polarizabilities were computed by using a series of methods, HF, MP2, coupled cluster, which involves the iterative computation of single and double excitation amplitudes (CCSD), as well as the perturbative treatment of triples excitations (CCSD(T)),[47] with the aug-cc-pVNZ (N = D,T,Q,5) basis sets.[48] For Xe, we use the small-core relativistic effective potential of Ref. [48], with 28 core electrons, together with corresponding basis sets aug-cc-pVNZ-PP (PP: Pseudo Potential). It has been reported that effective core potentials can give reliable (hyper)polarizability values.[49]

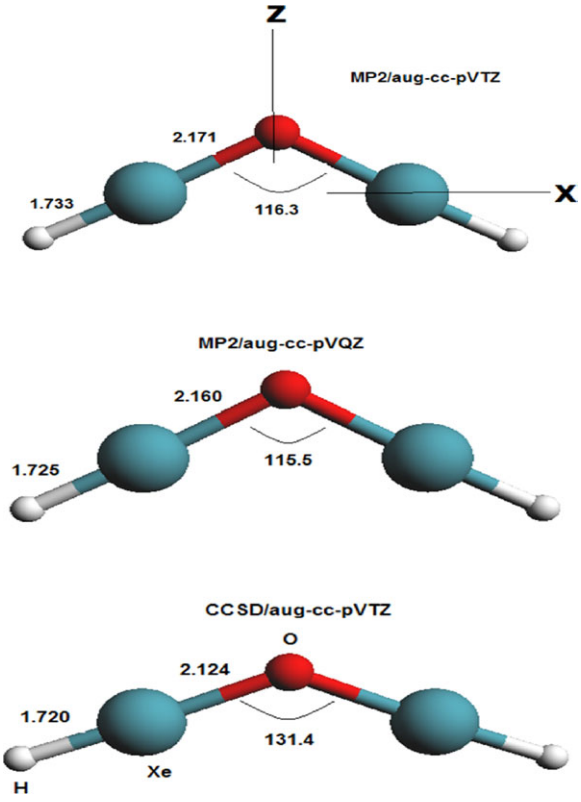

Figure 1. Bond lengths (Å) and angles (degrees) of HXeOXeH.

Vibrational L&NLO properties

The vibrational contributions to (hyper)polarizabilities can be of significant importance.[42] Several methods have been developed for their computation, using, for example, vibrational self-consistent field theory and correlated versions.[50,51] Bishop and Kitrman[42a–d] introduced several techniques for the computation of the vibrational L&NLO properties among which we

note those which are based on perturbation theory, and the finite field nuclear relaxation (nr) approach developed by Bishop et al.[52] and implemented by Luis et al.[53] In the latter approach, the molecular geometry is optimized in the presence of static electric fields rigorously enforcing the Eckart conditions.[54] The method requires the computation of the energy in the presence of a uniform static electric field F, allowing the nuclei to relax to field-dependent equilibrium positions. By denoting R_0 and R_F, the equilibrium geometries with $F = 0$ and $F \neq 0$, respectively, one may write the difference of the property $\Delta P_{R(F)} = P^e[R_F,F] - P^e[R_0,0]$, $P = E,\mu,\alpha,\beta$ as a Taylor expansion in the field. If $P = E$ (energy) the expansion may be written as:

$$\Delta E_{R(F)} = b_1F_i + \frac{1}{2}b_2F_iF_j + \frac{1}{6}b_3F_iF_jF_k + \frac{1}{24}b_4F_iF_jF_kF_l + \ldots\ldots, \quad (2)$$

where i,j,k,l denote Cartesian axes. The coefficients b_n, $n = 1,2,3,4$ correspond to the total value of the nth-order property:

$$b_1 = [\mu_i(0)]^{el} + [\mu_i(0)]^{nr} \quad (3)$$

$$b_2 = [\alpha_{ij}(0;0)]^{el} + [\alpha_{ij}(0;0)]^{nr} \quad (4)$$

$$b_3 = [\beta_{ijk}(0;0,0)]^{el} + [\beta_{ijk}(0;0,0)]^{nr} \quad (5)$$

$$b_4 = [\gamma_{ijkl}(0;0,0,0)]^{el} + [\gamma_{ijkl}(0;0,0,0)]^{nr} \quad (6)$$

where the frequency argument "0" denotes static (hyper)polarizabilities. The nr vibrational contribution to dipole moment is zero. The static nr vibrational (hyper)polarizabilities [eqs. (4)–(6)] can also be derived by using the corresponding Taylor expansion of the change of the dipole moment ($\Delta\mu(F,R_F)$) in the field.[42d] If one uses in expansion (2) instead of the energy the corresponding polarizability change ($\Delta\alpha(F,R_F)$) or the change of the first hyperpolarizability ($\Delta\beta(F,R_F)$), the procedure allows the computation of dynamic vibrational nr contributions in the infinite optical frequency approximation (IOFA).[42a]

In terms of perturbation theory, named as Bishop–Kirtman perturbation theory (BKPT), the average and diagonal components of nr vibrational contributions (static and dynamic) are given by the following analytical formulas:[40–42d]

$$\alpha^{nr}(0;0) = [\mu^2]^{(0,0} \quad (7)$$

$$\beta^{nr}(0;0,0) = [\mu\alpha]^{(0,0)} + [\mu^3]^{(1,0)} + [\mu^3]^{(0,1)} \quad (8)$$

$$\gamma^{nr}(0;0,0,0) = [\alpha]^{(0,0)} + [\mu\beta]^{(0,0)} + [\mu^2\alpha]^{(1,0)} + [\mu^2\alpha]^{(0,1)} + [\mu^4]^{(2,0)} + [\mu^4]^{(1,1)} + [\mu^4]^{(0,2)} \quad (9)$$

$$\beta(-\omega;\omega,0,0)_{\omega->\alpha} = \frac{1}{3}[\mu a]^{(0,0)}_{\omega=0} \quad (10)$$

$$\gamma^{nr}(-\omega;\omega,0,0)_{\omega->\alpha} = \frac{1}{3}[\alpha^2]^{(0,0)}_{\omega=0} + \frac{1}{2}[\mu\beta]^{(0,0)}_{\omega=0} + \frac{1}{6}([\mu^2\alpha]^{(1,0)} + [\mu^2\alpha]^{(0,1)} \quad (11)$$

$$\gamma^{nr}(-2\omega;\omega,\omega,0)_{\omega->\alpha} = \frac{1}{4}[\mu\beta]^{(0,0)}_{\omega=0} \quad (12)$$

The superscripts n and m in the notation $[A]^{n,m}$, denote the level of the electrical and mechanical anharmonicities, respectively. The above equations for the computation of the vibrational dynamic hyperpolarizabilities imply the IOFA, which requires that for all vibrational transition frequencies (ω_t) and optical frequencies (ω), the ratio $(\omega_t/\omega)^2$ is negligible compared to unity.[42d] According to eqs. (7)–(12), all vibrational contributions through first-order in mechanical and/or electrical anharmonicity and some of the second-order terms are included in the finite field nr approach. Higher-order vibrational corrections, which are called curvature contributions, are usually smaller and their computation is very time-consuming.[55] They will not be considered in this study.

The geometries used for the computation of the nr vibrational properties of the reported Xe derivatives were optimized using MP2 and CCSD with the aug-cc-pVXZ (X = T,Q) basis sets, without imposing symmetry constraints. All the Xe derivatives considered in this study are planar, and are placed in the XZ plane (Fig. 1). In the context of the finite field nr method, field strengths from 0.0008 to 0.0064 a.u were used in the Eckart constrained optimizations, applied along the x and z axis only. Only the energies of the optimized structures were analyzed by using a numerical Romberg differentiation[46] in order to ensure the numerical stability of the results.

The zero point vibrational averaging (ZPVA) contributions to α and β presented in this work were computed using the BKPT.[40,42] This correction provides a part of the curvature contribution which arises from the change of the zero point vibrational energy caused by the applied field. According to BK perturbation theory, the ZPVA correction is evaluated as a double perturbation series in mechanical and electrical anharmonicity and is given by a sum of the nonvanishing odd order terms,[42d]

$$P^{ZPVA} = [P]^{I} + [P]^{III} + \ldots, \quad (13)$$

where P denotes the electronic property (μ,α,β,γ), $[P]^{I} = [P]^{(1,0)} + [P]^{(0,1)}$, while $[P]^{III} = [P]^{(3,0)} + [P]^{(2,1)} + [P]^{(1,2)} + [P]^{(0,3)}$ where (n,m) superscripts stand for the order of the electrical and mechanical anharmonicity contribution, respectively. The first-order term is given by

$$[P^{zpva}]^{I} = -\frac{\hbar}{4}\sum_a \frac{1}{\omega_a^2}\left(\sum_b \frac{F_{abb}}{\omega_b}\right)\left(\frac{\partial P^e}{\partial Q_a}\right) + \frac{\hbar}{4}\sum_a \frac{1}{\omega_a}\left(\frac{\partial^2 P^e}{\partial Q_a^2}\right) \quad (14)$$

where $P = \alpha,\beta$, F_{abb} denotes the cubic force constant, and ω_a the harmonic vibrational frequency of the normal mode Q_a. The purpose of our first-order ZPVA calculations is to check if the sequence P^e, $[P]^{I}$, $[P]^{III}$ is initially convergent (i.e., $[P]^{I} < P^e$).[42d] The evaluation of the higher-order ZPVA [eq. (13)] and other higher-order curvature terms requires the computation of higher-order force constants and electronic property derivatives. For convergent P^e, $[P]^{I}$, and $[P]^{III}$ series, the higher-order vibrational terms are usually very small. Furthermore, their computation is very time consuming and then they were not considered in this study. The cubic force constants used in eq. (14) were computed numerically as first derivatives of the analytical force constants, while the derivatives $\frac{\partial^2 P^e}{\partial Q_a^2}$ were computed numerically from the corresponding properties.

Software. The GAUSSIAN 09 software[56] has been used for the optimization and (hyper)polarizability computations with the

Table 1. Basis set study of the static electronic (hyper)polarizabilities of HXeOXeH. The properties have been computed by employing the MP2 method at the MP2/aug-cc-pVQZ optimized geometry.

Basis set: aug-cc-pVNZ[a] property[b]	N			
	D	T	Q	5[c]
α_{xx}	177.86	180.43 181.37[d]	181.96 182.26[e]	182.63
α_{zz}	72.27	74.29 75.14[d]	75.52 74.96[e]	74.73
β_{zzz}	4.1	11.7 45.3[d]	36.6 50.3[e]	39.2
γ_{xxxx}	26.94×10^3	19.73×10^3 52.70×10^3[d]	35.11×10^3 51.50×10^3[e]	46.0×10^3
γ_{zzzz}	16.74×10^3	21.69×10^3 32.89×10^3[d]	27.81×10^3 34.04×10^3[e]	30.0×10^3

All property values are given in a.u.
[a] For Xe, the small-core relativistic effective potential of Ref. [48] with 28 core electrons was used. [b] Polarizability derivatives were used for the computation of the reported tensor components. [c] Energy derivatives were used for the computation of the reported tensor components. [d] Basis set: daug-cc-pVTZ. [e] Basis set: daug-cc-pVQZ.

aug-cc-pVNZ basis sets, where N = D, T, and Q. NWCHEM[57] was used for the computation of the (hyper)polarizabilities employing the aug-cc-pV5Z basis set.

Results and Discussion

Electronic (hyper)polarizabilities

As the computation of the vibrational (hyper)polarizabilities depends on the electronic properties, we have performed a limited study of the dependence of the electronic contribution on the basis set, electron correlation and geometry.

Basis set effect. The effect of the basis set on the static electronic (hyper)polarizabilities of HXeOXeH is presented in Table 1. The study has been performed at the MP2 level using the MP2/aug-cc-pVQZ geometry. For all computations the (d)-aug-cc-pVNZ basis set series has been used, where N = D,T,Q,5. It is seen that the basis set has a large effect on the electronic first and second hyperpolarizabilites. For example, γ_{xxxx} increases by 70.7% by switching from aug-cc-pVDZ to aug-cc-pV5Z. The effect on the polarizability components is significantly smaller where the α_{xx} is increased by 2.7%. Even between the largest basis sets, aug-cc-pVQZ and aug-cc-pV5Z, the hyperpolarizabilities differ substantially, where an increase of 31% is observed for γ_{xxxx}. The substantial change of γ_{xxxx} upon basis set change implies that the use of aug-cc-pVNZ basis sets may not be adequate for a proper basis set limit estimation of the property. We also computed the diagonal in-plane (hyper)polarizability values by using the d-aug-cc-pVNZ basis set series for H, C, O atoms, where N = T,Q.[58] For Xe, we use the small-core relativistic effective potential of Ref. [48], with 28 core electrons, together with corresponding basis sets aug-cc-pVNZ-PP augmented with extra diffuse functions.[48] A very large basis set effect is observed for the first and second hyperpolarizability values (Table 1) when the second set of diffuse functions are added to the basis set. It is seen that γ_{xxxx} (d-aug-cc-pVTZ) $=2.67 \times \gamma_{xxxx}$(aug-cc-pVTZ), while γ_{xxxx}(d-aug-cc-pVQZ) $= 1.47 \times \gamma_{xxxx}$(aug-cc-pVQZ). Noticeable is also the effect on the first hyperpolarizability (e.g., β_{zzz}(d-aug-cc-pVQZ) $= 1.37 \times \beta_{zzz}$(aug-cc-pVQZ)). Contrary to the single augmented series, the hyperpolarizabilities can be considered converged at the d-aug-cc-pVTZ basis set. It is seen that γ_{xxxx}(d-aug-cc-pVQZ) changes only by 2.2% with respect to γ_{xxxx}(d-aug-cc-pVTZ).

Electron correlation. For all studied geometries, the electron correlation effect is larger for the x diagonal tensor component of the second hyperpolarizability than for the z diagonal component (Table 2). It is observed that electron correlation at the CCSD(T) level decreases the γ_{xxxx}(HF) value by 38.5%, 51.1%, and 57.1%, for the geometries, CCSD/aug-cc-pVTZ and MP2/aug-cc-pVQZ, MP2/aug-cc-pVTZ, respectively. Similarly, the effect of electron correlation (CCSD(T)) on the γ_{zzzz} diagonal component increases the HF value by 41%, computed at the MP2/aug-cc-pVQZ geometry. The effect of the pertubatively computed triples correction is significant on the diagonal x tensor component of the second hyperpolarizability, for example, γ_{xxxx} (CCSD(T)) $-$ γ_{xxxx} (CCSD) $= -15.7 \times 10^3$ a.u., (CCSD/aug-cc-pVTZ geometry).

Geometry effect. The effect of the change of the geometry on the second hyperpolarizability is quite large (Table 2). For example, it was found that γ_{xxxx} at the CCSD(T)/aug-cc-pVTZ level of theory of the structure optimized at MP2/aug-cc-pVQZ differs by 37.7% from the structure optimized at the CCSD/aug-cc-pVTZ level, while for the z-component the above difference is 37.4%. Even more pronounced is the geometry effect on the second hyperpolarizability at the MP2/aug-cc-pVTZ level theory. For example, we find that the MP2 γ_{xxxx}(MP2/aug-cc-pVQZ) value differs by 77% from the γ_{xxxx}(CCSD/aug-cc-

Table 2. A study of the geometry and the electron correlation effect on the static electronic polarizability and second hyperpolarizability ($\times 10^3$) of HXeOXeH. All the reported values were computed by employing the aug-cc-pVTZ[a] basis set, while the geometries have been optimized by using the specified method.

Optimized geometry property (a.u.)[b]	MP2/aug-cc-pVTZ				CCSD/aug-cc-pVTZ				MP2/aug-cc-pVQZ			
	α_{xx}	α_{zz}	γ_{xxxx}	γ_{zzzz}	α_{xx}	α_{zz}	γ_{xxxx}	γ_{zzzz}	α_{xx}	α_{zz}	γ_{xxxx}	γ_{zzzz}
HF	176.89	68.42	154.4	13.5	181.05	62.16	184.0	9.60	171.31	68.41	144.0	13.52
MP2	185.24	74.26	1.97	21.5	196.56	64.79	85.5	14.90	180.43	74.29	19.6	21.60
CCSD	183.41		78.6		190.69	62.70	128.7	12.35	178.05	71.29	81.0	17.30
CCSD(T)	183.34		66.0		192.99	63.62	113.0	13.90	178.40	72.23	70.4	19.10

[a] For Xe an effective core potential of 28 electrons was used.[48] [b] Energy derivatives were used for the computation of the reported tensor components.

pVTZ) (in parenthesis, the level of the geometry optimization is given), while the γ_{xxxx}(MP2/aug-cc-pVTZ) differs by 97.6% from the corresponding γ_{xxxx}(CCSD/aug-cc-pVTZ). Similarly, the γ_{xxxx}(MP2/aug-cc-pVTZ) value differs by 89.9% from the γ_{xxxx}(MP2/aug-cc-pVQZ) value. Significantly smaller is the effect of geometry on the diagonal *z* component of the second hyperpolarizability. For example, it is seen that the γ_{zzzz}(MP2/aug-cc-pVQZ) value differs by 37.4% from the corresponding γ_{xxxx}(CCSD/aug-cc-pVTZ).

In Figure 1, the bond lengths, R_{O-Xe}, R_{H-Xe} and the angle <XeOXe of HXeOXeH, optimized at the MP2 and CCSD levels with the aug-cc-pVNZ, N = T,Q, basis sets are shown. The effect of the basis set on these geometries at the same level of theory is small: ΔR_{O-Xe}(MP2/BS1-MP2/BS2) = 0.011 Å, ΔR_{H-Xe}(MP2/BS1-MP2/BS2) = 0.008 Å, where BS1 and BS2 are the aug-cc-pVTZ and aug-cc-pVQZ basis sets, respectively. Similarly, the difference in <XeOXe angles is only 0.8° upon basis set change. However, going from MP to CCSD remarkable changes on the geometry parameters of HXeOXeH are observed, especially for the angle <XeOXe. The following differences will be later used to qualitatively explain the correlation effect on the NLO properties: ΔR_{O-Xe}(MP2/BS1-CCSD/BS1) = 0.047 Å, ΔR_{H-Xe}(MP2/BS1-CCSD/BS1) = 0.013 Å, and $\Delta\varphi_{<XeOXe}$ = (MP2/BS1-CCSD/BS1)= −15.1°.

In Figure 2, the variation of the γ_{xxxx} with the angle <XeOXe is shown. It is seen that the effect of the change of the angle

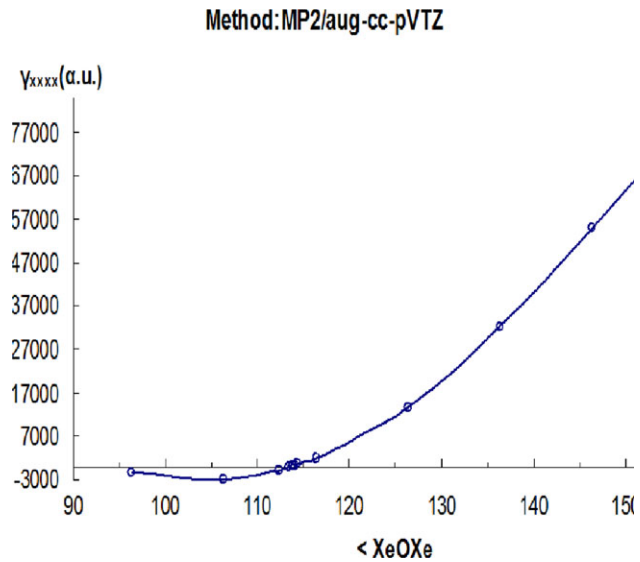

Figure 2. The dependence of γ_{xxxx} (electronic contribution) of HXeOXeH on the angle of XeOXe (degrees).

on the γ_{xxxx} is significant and thus the angle alone can be used to qualitatively explain the differences observed due to the change of geometry (Table 2).

From the above limited study, we may conclude that both basis set (Table 1) and electron correlation effects (Table 2) are quite important for the reliable estimation of the electronic (hyper)polarizabilities of the molecules studied here. These results are in agreement with Ref. [38]. The change of the geometry due to the effect of either electron correlation or basis set (Fig. 1) leads to a substantial variation of the second hyperpolarizability (Table 2, Fig. 2). Although the MP2 geometries differ substantially from the more accurate CCSD geometries, due to computational restrictions the former will be used in the subsequent computations, which should be sufficient for a qualitative estimation and analysis of the magnitude of the vibrational (hyper)polarizabilities. The previous findings will assist us to study thoroughly the vibrational (hyper)polarizabilities.

Vibrational (hyper)polarizabilities

Basis set effect. In order to examine the effect of basis set on the nr vibrational (hyper)polarizabilities, the HXeOXeH molecule was selected as a test molecule. For both methods, BKPT (Table 3) and the numerical finite field nr (Supporting Information Table S1), the basis set effect at the MP2 level of theory was found to be small on the nr contribution of α_{xx} and α_{zz} (MP2/aug-cc-pVXZ, X = T,Q). A small, but not negligible effect is also observed for most of the nr first and second hyperpolarizabilities, with the exception of. $\gamma_{zzzz}(-2\omega;\omega,\omega,0)$, where the change is large, but the value of this property is small anyway. The small basis set effect on the nr (hyper)polarizabilities may be explained by the concomitantly small changes of the geometry parameters (bond length and <XeOXe angle, Fig. 1) of HXeOXeH, computed at the MP2 level with the aug-cc-pVXZ basis sets, where X = T,Q. For the static and IOFA dynamic second hyperpolarizabilities, the results show a good convergence with respect to the basis set size, with relative differences for the *x* diagonal component (the largest) smaller than 7%. We

Table 3. Basis set study of the static electronic (El) (hyper)polarizabilities, static and IOFA dynamic nuclear relaxation (NR) vibrational contributions to the polarizability, first and second hyperpolarizability of HXeOXeH[a].

Method	MP2/aug-cc-pVTZ		MP2/aug-cc-pVQZ	
Property[b]	NR[c]	El	NR[c]	El.
$\alpha_{xx}(0;0)$	79.09 80.57[d]	185.24 187.70[e]	80.89	181.96
$\alpha_{yy}(0;0)$	0.58	54.90	0.57	55.30
$\alpha_{zz}(0;0)$	10.66	74.26	11.23	74.72
$\beta_{zzz}(0;0,0)$	−1390	7.3	−1425	36.6
$\beta_{zzz}(-\omega;\omega,0)$	−487		−506	
$\gamma_{xxxx}(0;0,0,0)$	1640×10^3 1970×10^3[d]	1.97×10^3 43.46×10^3[e]	1630×10^3	35.11×10^3
$\gamma_{yyyy}(0;0,0,0)$	0.53×10^3		0.42×10^3	
$\gamma_{zzzz}(0;0,0,0)$	95.4×10^3	21.50×10^3	95.5×10^3	27.81×10^3
$\gamma_{xxxx}(-\omega;\omega,0,0)$	186.0×10^3		199.0×10^3	
$\gamma_{yyyy}(-\omega;\omega,0,0)$	0.014×10^3		-0.049×10^3	
$\gamma_{zzzz}(-\omega;\omega,0,0)$	33.4×10^3		30.3×10^3	
$\gamma_{xxxx}(-2\omega;\omega,\omega,0)$	-107×10^3		-101×10^3	
$\gamma_{yyyy}(-2\omega;\omega,\omega,0)$	-0.13×10^3		-0.17×10^3	
$\gamma_{zzzz}(-2\omega;\omega,\omega,0)$	0.32×10^3		$0.053 - 10^3$	

All values are given in a.u.
[a] The molecule is placed in the *XZ* plane. [b] β_{xxx} and β_{yyy} are zero by symmetry. [c] The Bishop–Kirtman perturbation theory approach has been used for the computation of the nr contribution. [d] The nr values were computed by employing the finite field approach with the MP2/daug-cc-pVTZ method. [e] Method: MP2/daug-cc-pVTZ.

Table 4. Static electronic (El) (hyper)polarizabilities, static and IOFA dynamic nuclear relaxation (NR) vibrational contributions of the polarizability, first and second hyperpolarizability of HXeOXeH, HXeOXeF, and FXeOXeF.

Method	MP2/aug-ccpVTZ					
Compound[a]	HXeOXeH		HXeOXeF		FXeOXeF	
Property[b]	NR[c]	El	NR[c]	El	NR[c]	El
$\alpha_{xx}(0;0)$	79.09 (140.02)[d]	185.24 (190.69)[e]	112.02	150.33	56.05	138.02
$\alpha_{yy}(0;0)$	0.58	54.90	14.66	51.11	12.47	49.09
$\alpha_{zz}(0;0)$	10.66	74.26	13.56	66.14	28.02	64.37
$\beta_{zzz}(0;0,0)$	−1390	7.3	283	−22	886	−77
$\beta_{xxx}(-\omega;\omega,0)$	−1		−1248		0	
$\beta_{yyy}(-\omega;\omega,0)$	−0.02		0.01		0	
$\beta_{zzz}(-\omega;\omega,0)$	−487		44		390	
$\gamma_{xxxx}(0;0,0,0)$	1640×10^3 (2790×10^3)[d]	1.97×10^3 (128.70×10^3)[e]	2159×10^3	64.45×10^3	633×10^3	-12.69×10^3
$\gamma_{yyyy}(0;0,0,0)$	0.53×10^3		13.8×10^3		4.7×10^3	
$\gamma_{zzzz}(0;0,0,0)$	95.4×10^3	21.50×10^3	81.2×10^3	11.64×10^3	37.1×10^3	6.92×10^3
$\gamma_{xxxx}(-\omega;\omega,0,0)$	186.0×10^3		79.2×10^3		102.6×10^3	
$\gamma_{yyyy}(-\omega;\omega,0,0)$	0.014×10^3		1.1×10^3		0.14×10^3	
$\gamma_{zzzz}(-\omega;\omega,0,0)$	33.4×10^3		19.4×10^3		1.21×10^3	
$\gamma_{xxxx}(-2\omega;\omega,\omega,0)$	-107×10^3		-93.7×10^3		-5.65×10^3	
$\gamma_{yyyy}(-2\omega;\omega,\omega,0)$	-0.13×10^3		-0.62×10^3		-0.69×10^3	
$\gamma_{zzzz}(-2\omega;\omega,\omega,0)$	0.32×10^3		-0.80×10^3		-3.05×10^3	

All values are in a.u.

[a] The molecule is placed in the *XZ* plane. [b] β_{xxx} and β_{yyy} of HXeOXeH and FXeOXeF, and β_{yyy} of HXeOXeF are zero by symmetry. [c] The Bishop–Kirtman perturbation theory approach has been used for the computation of the nr contribution. [d] The nr values were computed by employing the finite field approach with the CCSD/aug-cc-pVTZ method. [e] Method: CCSD/aug-cc-pVTZ.

have also computed the static nr γ_{xxxx} component by using the d-aug-cc-pVTZ basis set. It is seen that the reported γ_{xxxx}(MP2/aug-cc-pVTZ) nr value differs by 16.7% from the γ_{xxxx}(MP2/d-aug-cc-pVTZ) one. On the contrary, the basis set effect on the electronic hyperpolarizabilities is considerable larger (see Basis set effect section).

Electron correlation effect. In order to examine the effect of electron correlation on the nr (hyper)polarizabilities, the HXeOXeH molecule was selected as a test case. The reported results (Table 4) were computed by using BKPT approach on the MP2 results and the finite field nr approach for the CCSD/aug-cc-pVTZ data. We have restricted our CCSD computations to the diagonal *x*-component of the vibrational polarizability and second hyperpolarizability, as this component is dominant for all the studied Xe derivatives (Table 4). It is observed that electron correlation has a significant effect on the nr contribution of α_{xx} and γ_{xxxx}. It was found that the α_{xx} (MP2) differs by 43.5% from α_{xx} (CCSD), while γ_{xxxx} (MP2) differs by 41.2% from γ_{xxxx}(CCSD). Again, this large effect may be explained by the corresponding differences in the optimized geometries due to the effect of electron correlation, as computed by the MP2/aug-cc-pVTZ and CCSD/aug-cc-pVTZ, methods (Fig. 1). It is interesting to note that comparison between the CCSD and MP2 values shows that MP2 is able to estimate the correct order of magnitude for the nr second hyperpolarizability. However, this is not valid for the electronic second hyperpolarizability as shown in the results of Tables 2 and 4. The nuclear relaxation contributions to the second hyperpolarizabilities depend on the derivatives respect to the normal modes of electronic low order properties [see eqs. (9), (11), and (12)]. The better performance of MP2 describing such properties decreases the difference between MP2 and CCSD nr second hyperpolarizabilities with respect to the large difference of their electronic counterparts. We conclude (section Geometry Effect) that the geometry is not greatly affected by the basis set, but a remarkable effect is observed due to electron correlation. The nr contributions to α_{xx} and γ_{xxxx} are also significantly affected by electron correlation and in a lesser extent by the basis set. These results imply a direct connection between the geometry changes and the changes of the nr contributions. This is in agreement with the results of Ref. [59].

Nuclear relaxation (hyper)polarizabilities. The results for the nr vibrational contributions to the L&NLO properties of the selected Xe derivatives are reported in Table 4. All the reported results and subsequent analysis for the *nr* (hyper)polarizabilites were computed at the MP2 level theory. It was shown that at this level the order of magnitude is correct compared with the more accurate CCSD value. Thus, a qualitatively analysis at MP2 level can be performed in order to comment on the magnitude of the nr vibrational (hyper)polarizabilities of the studied rare gas derivatives.

We have checked our BKPT results with those computed by the finite field method and the agreement is very good (Table 4 and Supporting Information Table S2). Let us note that the finite field nr method works satisfactorily as long as the field-dependent optimized geometry corresponds to the same minimum as the field-free optimized one. This is valid for the HXeOXeH molecule (Fig. 3). It is seen that an applied field of 0.0064 a.u, along *x* or *z* direction, leads to small differences in the geometrical parameters of the field free optimized geometry (Fig. 1), where the largest difference is observed for the XeOXe angle (Figs. 1 and 3).

In general, the static nr contribution to the first- and second-order hyperpolarizability components is significantly larger

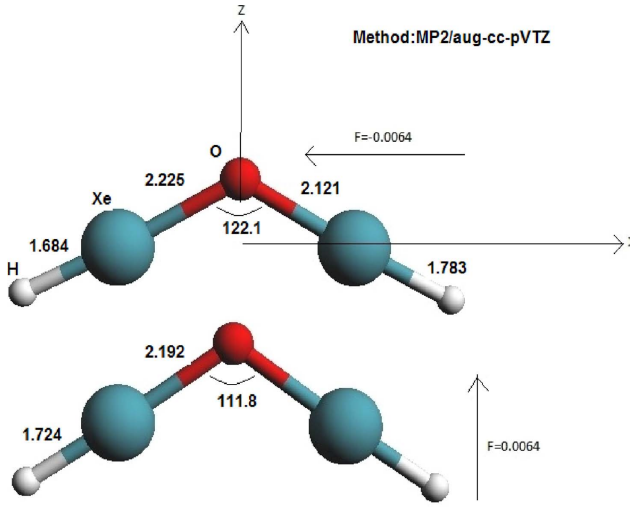

Figure 3. Bond lengths (Å) and angles (degrees) of field-dependent optimized geometries of HXeOXeH. [Color figure can be viewed in the online issue, which is available at wileyonlinelibrary.com.]

than the corresponding electronic ones for all the derivatives, especially for the second hyperpolarizability. In order to quantify this, we will analyze the ratio P^{nr}/P^{el} at the MP2/aug-cc-pVTZ level. For β_{xxx} (HXeOXeF), this ratio takes the value −6.24 (Supporting Information Table S2), for γ_{xxxx}, the ratio is 832.4, 33.5, and −49.9, for HXeOXeH, HXeOXeF, and FXeOXeF, respectively. For β_{zzz}, the P^{nr}/P^{el} is −190 (HXeOXeH), −12.9 (HXeOXeF), −11.5(FXeOXeF), and for γ_{zzzz}, 4.4 (HXeOXeH), 6.9 (HXeOXeF), and 5.4 (FXeOXeF). The opposite was found for the polarizability, where for all the studied compounds it was found that $\alpha_{ii}^{el.} > \alpha_{ii}^{nr}$ $I = x,z$.

Let us now highlight some features observed for the computed nr contributions of the selected Xe derivatives. (a) A noticeable difference between the in-plane nr first hyperpolarizability components of HXeOXeF is found, $\beta_{xxx}(nr) - \beta_{zzz}(nr) = -10.53 \times 10^3$ a.u. (MP2/FF). (b) The differences, $\alpha_{xx}(nr) - \alpha_{zz}$ (nr) and γ_{xxxx} (nr) − γ_{zzzz} (nr) are largest for HXeOXeF (Table 4). (c) For the diagonal *x*-component, we found the sequence (Table 4) P^{nr}(HXeOXeF) > P^{nr}(HXeOXeH) > P^{nr}(FXeOXeF), where $P = \alpha, \beta, \gamma$. A somehow different pattern is observed for the diagonal *z*-component of the (hyper)polarizability tensor components: α^{nr}(FXeOXeF) > α^{nr}(HXeOXeF) > α^{nr}(HXeOXeH), $|\beta^{nr}$(HXeOXeH)| > $|\beta^{nr}$(FXeOXeF)| > $|\beta^{nr}$(HXeOXeF)|, γ^{nr}(HXeOXeH) > γ^{nr}(HXeOXeF) > γ^{nr}(FXeOXeF). (d) For all the studied compounds, at both static and dynamic level of theory, the out of plane vibrational (hyper)-polarizability component is smaller than the in-plane (Table 4), except for α_{yy}^{nr} of HXeOXeF, which is slightly larger than the α_{zz}^{nr}.

Summarizing, we found that the vibrational first and second hyperpolarizabilities of the three studied Xe derivatives are larger than the electronic ones, with an especially large ratio P^{nr}/P^{el} for the second hyperpolarizability. Interestingly, the γ_{xxxx}^{nr} component dominates and reaches a maximum value for HXeOXeF.

ZPVA (hyper)polarizabilites. We shall now comment on the ZPVA correction, at the MP2/aug-cc-pVTZ level of theory, for the polarizability and first hyperpolarizability. For the polarizability, the ratio $[\alpha^{ZPVA}]^I/\alpha^{el}$ for the diagonal in-plane components of the reported Xe derivatives, is always smaller than unity, implying that the series $P = P^{el} + [P^{ZPVA}]^I$ is convergent.[55,60]

For the *x* (*z*) diagonal component of the polarizability, the ratio $[\alpha^{ZPVA}]^I/\alpha^{el}$ is: 0.02 (0.02), 0.03 (0.01), and 0.008 (0.006), for HXeOXeH, HXeOXeF, and FXeOXeF, respectively. Similarly for the *x* (*z*) diagonal component of the first hyperpolarizability, the ratio $[\beta_{xxx}^{ZPVA}]^I/\beta_{xxx}^{el}$ is 0.05 (−0.12) and 0.04, for HXeOXeF and FXeOXeF, respectively.

Rationalization of the nr results. In this section, we will assess the origin of the computed large nr (hyper)polarizabilities on the basis of the BKPT theory, by comparing the contribution of various terms associated with given orders of mechanical and electrical anharmonicities. As, for all the studied Xe derivatives, the largest nr vibrational component is the *x* diagonal tensor component of the second hyperpolarizability (Table 4), our analysis will be restricted to this component by assessing the contribution of the following terms [eq. (9)]: $[\alpha^2]^0$, $[\mu\beta]^0$, $[\mu^2\alpha]^I$, $[\mu^4]^{II}$. The results are depicted in Figure 4 as a percentage of each contribution to the total value of γ_{xxxx}^{nr}. In order to facilitate our analysis, the various contributions have been grouped into harmonic ($[\alpha^2]^0 + [\mu\beta]^0$), first-order ($[\mu^2\alpha]^I = [\mu^2\alpha]^{(1,0)} + [\mu^2\alpha]^{(0,1)}$) and second-order ($[\mu^4]^{II} = [\mu^4]^{(2,0)} + [\mu^4]^{(1,1)} + [\mu^4]^{(0,2)}$) terms. It is seen that for the Xe derivatives, the harmonic approximation fails to provide the correct order of magnitude of the nr vibrational second hyperpolarizability (Fig. 4). Apart from the large magnitude of the anharmonic contribution, the failure of the harmonic approximation is also attributed to the partial cancellation of the relevant harmonic terms, which for HXeOXeF is quite large ($[\alpha^2]^0 = 3.19 \times 10^5$, $[\mu\beta]^0 = -3.75 \times 10^5$). The best performance of the harmonic approximation was found for FXeOXeF (25%). The anharmonicity has a similar weight for γ^{nr} of FXeOXeF and HXeOXeH. For HXeOXeH (FXeOXeF), the harmonic terms contribute 20% (25%), the first-order 55% (51%), and the second-order 25% (24%) to the total value (Table 4). The term which dominates the first-order contribution is $[\mu^2\alpha]^{(1,0)}$, with the values of 5.17×10^5, 8.1×10^5, and 4.01×10^5 for HXeOXeH, HXeOXeF, and FXeOXeF, respectively. This term is connected with dipole moment and polarizability second-order derivatives with respect to normal coordinates. For HXeOXeF, the major contribution (55%) to the total value originates from the second-order terms, where the $[\mu^4]^{(2,0)}$ is dominant (9.96×10^5 a.u) and is associated with higher-order dipole moment derivatives.[42c] Therefore, we conclude that the large contribution of the anharmonic terms and especially those connected with electrical anharmonicities[42c] are the reason for the high nr second hyperpolarizability values.

The effect of Xe insertion on the vibrational nonlinear optical properties

As shown previously, the insertion of an Ng atom leads to a substantial change of the electronic (hyper)polarizabilities.[37] Thus, it will be of interest to study the effect of Xe insertion on the nr vibrational (hyper)polarizabilities. The HXeOXeH, HXeOH, and H_2O will be used in order to address several features associated with the change of the vibrational properties

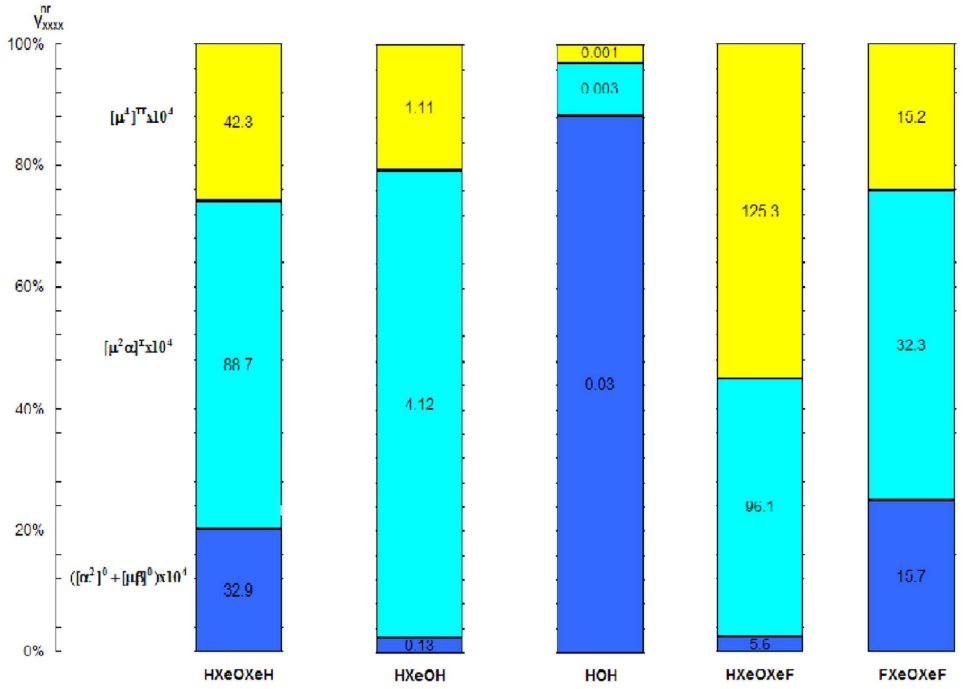

Figure 4. Analysis of the contribution of the harmonic and anharmonic terms to the γ^{nr}_{xxxx}. [Color figure can be viewed in the online issue, which is available at wileyonlinelibrary.com.]

upon Ng insertion. The results are reported in Table 5. In general, it is observed that the number of Xe atoms noticeably increases the magnitude of the nr contribution to the (hyper)-polarizabilities, at both static and dynamic levels. It has been shown that the MP2/aug-cc-pVTZ method gives the correct order of magnitude of the vibrational (hyper)polarizabilities, compared with the more accurate CCSD values. Thus, this method can be used to describe the effect of Xe insertion to the nr vibrational (hyper)polarizabilites at least qualitatively. The effect is largest for the *x* diagonal component of the polarizability and second hyperpolarizability. It was found that: α^{nr}_{xx}(HXeOXeH)/α^{nr}_{xx}(HOH) = 608.4 (14.4) a.u, γ^{nr}_{xxxx}(HXeOXeH)/γ^{nr}_{xxxx}(HOH) = 4823(477) a.u. In parenthesis, the ratio of the *z*-component is given.

The effect of Xe insertion is larger for the vibrational (hyper)polarizabilities than for the electronic ones. For example, for the *x*-component of the second hyperpolarizability, γ^{nr}_{xxxx}(HXeOXeH)/γ^{nr}_{xxxx}(HOH) = 4823 a.u, while γ^{el}_{xxxx}(HXeOXeH)/γ^{el}_{xxxx}(HOH) = 3.2a.u., γ^{nr}_{xxxx}(HXeOH)/γ^{nr}_{xxxx}(HOH) = 157 a.u, while γ^{el}_{xxxx}(HXeOH)/ γ^{el}_{xxxx}(HOH) = 43.9 a.u. Similar relationships were

Table 5. Static electronic (El.) (hyper)polarizabilities, static and IOFA dynamic nuclear relaxation (NR) vibrational contributions of the polarizability, first and second hyperpolarizability of HOH, HXeOH, and HXeOXeH.

Method	MP2/aug-cc-pVTZ					
Compound[a]	HXeOXeH		HXeOH		HOH	
Property[b]	NR[c]	El.	NR[c]	El.	NR[c]	El.
$\alpha_{xx}(0;0)$	79.09	185.24	22.01	70.63	0.13	10.01
$\alpha_{zz}(0;0)$	10.66	74.26	6.92	44.49	0.74	9.55
$\beta_{xxx}(0;0,0)$			−547.9	491.7		
$\beta_{zzz}(0;0,0)$	−1390	7.3	−136.8	79.0	−5.0	12.2
$\beta_{xxx}(-\omega;\omega,0)$			−121.3			
$\beta_{zzz}(-\omega;\omega,0)$	−487		−35.9		−3.1	
$\gamma_{xxxx}(0;0,0,0)$	1640×10^3	1.97×10^3	53.7×10^3	27.21×10^3	0.34×10^3	0.62×10^3
$\gamma_{zzzz}(0;0,0,0)$	95.4×10^3	21.54×10^3	13.1×10^3	9.68×10^3	0.20×10^3	1.09×10^3
$\gamma_{xxxx}(-\omega;\omega,0,0)$	186.0×10^3		0.38×10^3		0.10×10^3	
$\gamma_{zzzz}(-\omega;\omega,0,0)$	33.4×10^3		2.12×10^3		0.034×10^3	
$\gamma_{xxxx}(-2\omega;\omega,\omega,0)$	-107×10^3		-10.3×10^3		-0.006×10^3	
$\gamma_{zzzz}(-2\omega;\omega,\omega,0)$	0.32×10^3		-0.91×10^3		-0.014×10^3	

All values are in a.u.
[a] The molecule is placed in the *XZ* plane. The geometry of the derivatives has been optimized by using the MP2/aug-cc-pVTZ method. [b] β_{xxx} and β_{yyy} of HXeOXeH and HOH, and β_{yyy} of HXeOH are zero by symmetry. [c] The Bishop–Kirtman perturbation theory approach (BKPT) has been used for the computation of the nr contribution.

observed for the polarizability and first hyperpolarizability (Table 5).

In order to analyze the effect of Xe insertion on the nr vibrational (hyper)polarizabilities in more detail, we have studied the changes of various terms in the context of BKPT theory. Our analysis is restricted to the *x* diagonal component of nr second hyperpolarizability, as its contribution is the largest (Table 5). The results are depicted in Figure 4. As expected for H_2O, the major contribution to γ^{nr} originates from the harmonic term, associated with $[\alpha]^{(0,0)}$. The addition of one Xe atom (HXeOH) results in a remarkable increase of the first-order contribution, accounting for 77% of the total value, where the major effect originates from the $[\mu^2\alpha]^{(0,1)}$ term (6.29×10^4). The small effect of the harmonic contribution (less than 5%) for this molecule is due to the mutual cancellation of the relevant terms. The addition of the second Xe atom (HXeOXeH) has a large effect on all terms (Fig. 3), but especially on the anharmonic terms $[\mu^2\alpha]^{I}$ and $[\mu^4]^{II}$, which dominate the total value of the second vibrational hyperpolarizability. In conclusion, we may say that Xe insertion significantly affects the nr vibrational (hyper)polarizabilities at both static and dynamic levels, especially γ^{nr}_{xxxx}, due to the significant increase of the anharmonic terms (Fig. 4).

Conclusions

The goal of this study was to discuss the vibrational (hyper)polarizabilities of several noble gas derivatives. Three Xe derivatives, HXeOXeH, HXeOXeF, and FXeOXeF, known for their stability were used in order to investigate several features associated with the nr vibrational NLO properties. For their assessment, both BKPT and finite field nr methodologies were employed.

For the three studied derivatives, remarkably high nr vibrational (hyper)polarizabilities, especially second hyperpolarizabilities, were computed. The effect of electron correlation was found to be significant. A limited study on the HXeOXeH showed that the computed electronic and nr (hyper)polarizabilities are strongly affected by changes of the equilibrium geometry. An analysis based on the BKPT method revealed that the large values are due to the large contributions of the anharmonic terms, especially the electrical anharmonic ones (Fig. 4). The same trend was also observed for the dynamic nr properties, although these are considerably smaller than the static ones. However, they are still large in magnitude.

The effect of Xe insertion on the nr properties was also studied. The HOH, HXeOH, and HXeOXeH molecules were used. As expected, the harmonic terms dominate for the nr properties of H_2O. Addition of one Xe atom (HXeOH) remarkably changes the contribution of the first-order electrical and/or mechanical anharmonicity terms ($[\mu^2\alpha]^{I}$). Insertion of a second Xe atom (HXeOXeH) results in a significant increase of both first- and second-order terms of γ^{nr} (Fig. 4).

From the reported results, we may conclude that the anharmonic character of several vibrational modes in the Xe compounds[43,44] results in remarkable high vibrational (hyper)polarizabilities. Let us note that these compounds are unlikely to be useful as NLO materials. However, the present NLO results are useful, because they demonstrate a mechanism for designing molecules with very large hyperpolarizabilities. The efficient modeling of new NLO materials should take into account not only their electronic structure, but also their vibrational movements. Finally, a more rigorous study of the higher-order vibrational properties would require the use of methods as employed for the NH_3 molecule in Ref. [61] and will be the subject of a forthcoming study.

Acknowledgment

Grant in computing time by PRACE is gratefully acknowledged.

Keywords: (hyper)polarizabilities · noble gas compounds · vibrational contributions

How to cite this article: A. Avramopoulos, H. Reis, J. M. Luis, M. G. Papadopoulos, *J. Comput. Chem.* **2013,** *34,* 1446–1455. DOI: 10.1002/jcc.23280

Additional Supporting Information may be found in the online version of this article.

[1] N. Bartlett, D. Lohmann, *Proc. Chem. Soc.* **1962**, *115*, 5253.
[2] (a) R. Hoppe, W. Dahne, H. Mattauch, K. M. Rödder, *Angew. Chem.* **1962**, *74,* 903; (b) R. Hoppe, W. Dahne, H. Mattauch, K. M. Rödder, *Angew. Chem. Int. Ed. Engl.* **1962**, *1,* 599.
[3] G. M. Chaban, J. Lundell, R. B. Gerber, *Chem. Phys. Lett.* **2002**, *364,* 628.
[4] T. Ansbacher, R. B. Gerber, *Phys. Chem. Chem. Phys.* **2006**, *8,* 4175 and references therein.
[5] R. B. Gerber, *Annu. Rev. Phys. Chem.* **2004**, *55,* 55.
[6] J. O. C. Jiménez-Halla, I. Fernández, G. Frenking, *Angew. Chem. Int. Ed.* **2009**, *48,* 366.
[7] L. Khriachtchev, M. Pettersson, N. Runeberg, J. Lundell, M. Räsänen, *Nature* **2000**, *406,* 874.
[8] V. I. Feldman, F. F. Suhkov, *Chem. Phys. Lett.* **1996**, *255,* 425.
[9] M. Pettersson, L. Kriachtchev, A. Lignell, M. Räsänen, Z. Bihary, R. B. Gerber, *J. Chem. Phys.* **2002**, *116,* 2508.
[10] I. Last, T. F. George, *J. Chem. Phys.* **1998**, *89,* 3071.
[11] S. Berski, B. Silvi, J. Lundell, S. Noury, Z. Latajka, In New Trends in Quantum Chemistry in Physics and Chemistry; J. Marunai, C. Minot, R. McWeeny, Y. G. Smeyers, S. Wilson, et al. Eds.; Kluwer: Dordrecht, **2001**; p. 259.
[12] W. Grochala, *Chem. Soc. Rev.* **2007**, *36,* 1632.
[13] L. Khriachtchev, H. Tanskanen, J. Lundell, M. Pettersson, H. Kiljunen, M. Räsänen, *J. Am. Chem. Soc.* **2003**, *125,* 4696.
[14] V. I. Feldman, F. F. Sukhov, A. Y. Orlov, I. V. Tyulpina, I. V. *J. Am. Chem. Soc.* **2003**, *125,* 4698.
[15] H-J. Frohn, M. Theißen, *Ang. Chem. Int. Ed.* **2000**, *39,* 4591.
[16] M. Gerken, M. D. Moran, H. P. A. Mercier, B. E. Pointner, G. J. Schrobilgen, B. Hoge, K. O. Christe, J. A. Boatz, *J. Am. Chem. Soc.* **2009**, *131,* 13474.
[17] G. J. Schrobilgen, D. S. Brock, *J. Am. Chem. Soc.* **2011**, *133,* 6265.
[18] M. Pettersson, L. Khriachtchev, J. Lundell, M. Räsänen, *J. Am. Chem. Soc.* **1999**, *121,* 11904.
[19] L. Khriachtchev, M. Pettersson, J. Lundell, H. Tanskanen, T. Kiviniemi, N. Runeberg, M. Räsänen, *J. Am. Chem. Soc.* **2003**, *125,* 1454.
[20] K. Seppelt, S. Seidel, *Science* **2000**, *290,* 117.
[21] S. A. Cooke, M. C. L. Gerry, *J. Am. Chem. Soc.* **2004**, *43,* 3871.
[22] T. Arppe, L. Khriachtchev, A. Lignell, A. V. Domanskaya, M. Räsänen, *Inorg. Chem.* **2012**, *51,* 4398.
[23] (a) T. Drews, K. Seppelt, *Ang. Chem.* **1997**, *109,* 264; (b) T. Drews, K. Seppelt, *Ang. Chem. Int. Ed.* **1997**, *36,* 273.

[24] L. Khriachtchev, K. Isokoski, A. Cohen, M. Räsänen, R. B. Gerber, *J. Am. Chem. Soc.* **2008**, *130,* 6114.
[25] J. Lundell, L. Khriachtchev, M. Pettersson, M. Räsänen, *Chem. Phys. Lett.* **2004**, *388,* 228.
[26] (a) S. Borocci, N. Bronzolino, M. Giordani, F. Grandinetti, *J. Phys. Chem. A* **2010**, *114,* 7382; (b) S. Borocci, N. Bronzolino, F. Grandinetti, *Chem. Phys. Lett.* **2009**, *470,* 49.
[27] (a) E. Tsivion, S. Zilberg, R. B. Gerber, *Chem. Phys. Lett.* **2008**, *460,* 23; (b) E. Tsivion, R. B. Gerber, *Chem. Phys. Lett.* **2009**, *482,* 30; (c) G. M. Chaban, J. Lundell, R. B. Gerber, *Chem. Phys. Lett.* **2002**, *364,* 628.
[28] A. Krapp, G. Frenking, *Chem. Eur. J.* **2007**, *13,* 8256.
[29] Y. -L. Sun, J. -T. Hong, W. -P. Hu, *J. Phys. Chem. A.* **2010**, *114,* 9359.
[30] P. Antoniotti, E. Bottizzo, L. Operti, R. Rabezzana, S. Borocci, F. J. Grandinetti, *Phys. Chem. Lett.* **2010**, *1,* 2006.
[31] T.-H. Li, C.-H. Mou, H.-R. Chen, W.-P. Hu, *J. Am. Chem. Soc.* **2005**, *127,* 9241.
[32] G. Liu, H. Li, X. Zhang, W. Zhang, *Comput. Theor. Chem.* **2011**, *963,* 364.
[33] B. R. Wilson, K. Shi, A. K. Wilson, *Chem. Phys. Lett.* **2012**, *537,* 6.
[34] T. Jayasekharan, T. K. Ghanty, *J. Chem. Phys.* **2012**, *136,* 164312.
[35] R. Juarez, C. Zavala-Oseguera, J. Oscar, J. O. C. Jimenez-Halla, F. M. Bickelhaupt, G. Merino, *Phys. Chem. Chem. Phys.* **2011**, *13,* 2222.
[36] (a) A. Avramopoulos, H. Reis, J. Li, M. G. Papadopoulos, *J. Am. Chem. Soc.* **2004**, *126,* 6179; (b) A. Avramopoulos, L. Serrano-Andrés, J. Li, H. Reis, M. G. Papadopoulos, *J. Chem. Phys.* **2007**, *127,* 214102.
[37] A. Avramopoulos, L. Serrano-Andres, J. Li, M. G. Papadopoulos, *J. Chem. Theor. Comput.* **2010**, *6,* 3365.
[38] A. Avramopoulos, J. Li, N. Holzmann, G. Frenking, M. G. Papadopoulos, *J. Phys. Chem. A.* **2011**, *115,* 10226.
[39] J. Leszczynski, A. J. Sadlej, M. G. Papadopoulos, Non-Linear Optical Properties of Matter, Springer, The Netherlands, **2006**.
[40] D. M. Bishop, P. Norman, In Handbook of Advanced Electronic and Photonic Materials; H. S. Nalwa, Ed.; Academic Press: San Diego, **2000**.
[41] B. Kirtman, J. M. Luis, In Non-Linear Optical Properties of Matter; J. Leszczynski, A. J. Sadlej, M. G. Papadopoulos, Eds.; **2006**, pp. 101–129.
[42] (a) D. M. Bishop, B. Kirtman, *J. Chem. Phys.* **1991**, *95,* 2646; (b) D. M. Bishop, B. Kirtman, *J. Chem. Phys.* **1992**, *97,* 5255; (c) D. M. Bishop, J. M. Luis, B. Kirtman, *J. Chem. Phys.* **1998**, *108,* 10013; (d) B. Kirtman, B. Champagne, J. M. Luis, *J. Comp. Chem.* **2000**, *21,* 1572; (e) M. Garcia--Borras, M. Sola, J. M. Luis, B. Kirtman, *J. Chem. Theor. Comput.* **2012**, *8,* 2688; (f) V. E. Ingamells, M. G. Papadopoulos, S. G. Raptis, *Chem. Phys. Lett.* **1999**, *307,* 484; (g) U. Eckart, V. E. Ingamells, M. G. Papadopoulos, A. J. Sadlej, *J. Chem. Phys.* **2001**, *114,* 735; (h) A. Avramopoulos, V. E. Ingamells, M. G. Papadopoulos, A. J. Sadlej, *J. Chem. Phys.* **2001**, *114,* 198; (i) O. Loboda, R. Zalesny, A. Avramopoulos, J. M. Luis, B. Kirtman, N. Tagmatarchis, H. Reis, M. G. Papadopoulos, *J. Phys. Chem. A* **2009**, *113,* 1159.
[43] J. Lundell, G. M. Chaban, R. B. Gerber, *J. Phys. Chem. A* **2000**, *104,* 7944.
[44] Z. Bihary, G. M. Chaban, R. B. Gerber, *J. Chem. Phys.* **2002**, *116,* 5521.
[45] A. D. Buckingham, *Adv. Chem. Phys.* **1967**, *12,* 107.
[46] P. J. Davis, P. Rabinowitz, Numerical Integration; Blaisdell: London, **1967**; p. 166.
[47] R. J. Bartlett, In Advance Series in Physical Chemistry. Methods in Computational Chemistry, Vol. *2; D. R. Yarkony, Ed.; World Scientific: Singapore,* **1995**; p. 1047.
[48] K. A. Peterson, D. Figgen, E. Goll, H. Stoll, M. Dolg, *J. Chem. Phys.* **2003**, *119,* 11113.
[49] B. Jansik, B. Schimmelpfennig, P. Norman, P. Mochizuki, Y. Luo, H. Ågren, H. *J. Phys. Chem. A* **2002**, *106,* 395.
[50] O. Christiansen, *Phys. Chem. Chem. Phys.* **2007**, *9,* 2942.
[51] M. B. Hansen, O. Christiansen, C. Hattig, *J. Chem. Phys.* **2009**, *131,* 154101.
[52] D. M. Bishop, M. Hasan, B. Kirtman, *J. Chem. Phys.* **1995**, *103,* 4157.
[53] J. M. Luis, M. Duran, J. L. Andres, B. Champagne, B. Kirtman, *J. Chem. Phys.* **1999**, *111,* 875.
[54] C. Eckart, *Phys. Rev.* **1926**, *28,* 711.
[55] M. Torrent-Sucarrat, M. Sola, M. Duran, J. M. Luis, B. Kirtman, *J. Chem. Phys.* **2002**, *116,* 5363.
[56] M. J. Frisch, G. W. Trucks, H. B. Schlegel, G. E. Scuseria, M. A. Robb, J. R. Cheeseman, G. Scalmani, V. Barone, B. Mennucci, G. A. Petersson, H. Nakatsuji, M. Caricato, X. Li, H. P. Hratchian, A. F. Izmaylov, J. Bloino, G. Zheng, J. L. Sonnenberg, M. Hada, M. Ehara, K. Toyota, R. Fukuda, J. Hasegawa, M. Ishida, T. Nakajima, Y. Honda, O. Kitao, H. Nakai, T. Vreven, J. A. Montgomery, Jr., J. E. Peralta, F. Ogliaro, M. Bearpark, J. J. Heyd, E. Brothers, K. N. Kudin, V. N. Staroverov, R. Kobayashi, J. Normand, K. Raghavachari, A. Rendell, J. C. Burant, S. S. Iyengar, J. Tomasi, M. Cossi, N. Rega, J. M. Millam, M. Klene, J. E. Knox, J. B. Cross, V. Bakken, C. Adamo, J. Jaramillo, R. Gomperts, R. E. Stratmann, O. Yazyev, A. J. Austin, R. Cammi, C. Pomelli, J. W. Ochterski, R. L. Martin, K. Morokuma, V. G. Zakrzewski, G. A. Voth, P. Salvador, J. J. Dannenberg, S. Dapprich, A. D. Daniels, O. Farkas, J. B. Foresman, J. V. Ortiz, J. Cioslowski, D. J. Fox, Gaussian 09, revision A.02; Gaussian, Inc.: Wallingford, CT, **2009**.
[57] M. Valiev, E. J. Bylaska, N. Govind, K. Kowalski, T. P. Straatsma, H. J. J. van Dam, D. Wang, J. Nieplocha, E. Apra, T. L. Windus, W. A. de Jong, *Comput. Phys. Commun.* **2010**, *181,* 1477.
[58] T. H. Dunning, Jr., *J. Chem. Phys.* **1989**, *90,* 1007.
[59] V. E. Ingamells, M. G. Papadopoulos, A. J. Sadlej, *Chem. Phys. Lett.* **2000**, *260,* 1.
[60] (a) M. Torrent-Sucarrat, M. Sola, M. Duran, J. M. Luis, B. Kirtman, B. *J. Chem. Phys.* **2004**, *120,* 6346; (b) M. Torrent-Sucarrat, J. M. Luis, B. Kirtman, *J. Chem. Phys.* **2005**, *121,* 204108.
[61] J. M. Luis, H. Reis, M. G. Papadopoulos, B. Kirtman, *J. Chem. Phys.* **2009**, *131,* 034116.

Received: 9 November 2012
Revised: 4 March 2013
Accepted: 5 March 2013
Published online on 3 April 2013